Astron. Astrophys. 329, 971–985 (1998)

ASTRONOMY AND ASTROPHYSICS

The HIPPARCOS Hertzsprung-Russell diagram of S stars: probing nucleosynthesis and dredge-up⋆

S. Van Eck[1], **A. Jorissen**[1], **S. Udry**[2], **M. Mayor**[2], **and B. Pernier**[2]

[1] Institut d'Astronomie et d'Astrophysique, Université Libre de Bruxelles, C.P. 226, Boulevard du Triomphe, B-1050 Bruxelles, Belgium
[2] Observatoire de Genève, 51 Chemin des Maillettes, CH-1290 Sauverny, Switzerland

Received 23 May 1997 / Accepted 29 July 1997

Abstract. HIPPARCOS trigonometrical parallaxes make it possible to compare the location of Tc-rich and Tc-poor S stars in the Hertzsprung-Russell (HR) diagram: Tc-rich S stars are found to be cooler and intrinsically brighter than Tc-poor S stars.

The comparison with the Geneva evolutionary tracks reveals that the line marking the onset of thermal pulses on the asymptotic giant branch (AGB) matches well the observed limit between Tc-poor and Tc-rich S stars. Tc-rich S stars are, as expected, identified with thermally-pulsing AGB stars of low and intermediate masses, whereas Tc-poor S stars comprise mostly low-mass stars (with the exception of 57 Peg) located either on the red giant branch or on the early AGB. Like barium stars, Tc-poor S stars are known to belong exclusively to binary systems, and their location in the HR diagram is consistent with the average mass of 1.6 ± 0.2 $M_{\odot}$ derived from their orbital mass-function distribution (Jorissen et al. 1997, A&A, submitted).

A comparison with the S stars identified in the Magellanic Clouds and in the Fornax dwarf elliptical galaxy reveals that they have luminosities similar to the galactic Tc-rich S stars. However, most of the surveys of S stars in the external systems did not reach the lower luminosities at which galactic Tc-poor S stars are found. The deep Westerlund survey of carbon stars in the SMC uncovered a family of faint carbon stars that may be the analogues of the low-luminosity, galactic Tc-poor S stars.

Key words: stars: AGB – H-R diagram – stars: evolution – stars: fundamental parameters – stars: carbon

1. Introduction

The S stars are late-type giants whose spectra resemble those of M giants, with the addition of distinctive molecular bands of ZrO (Merrill 1922). Detailed abundance analyses of S stars (e.g., Smith & Lambert 1990) have shown that the overabundance pattern for the elements heavier than Fe bears the signature of the s-process nucleosynthesis (see Käppeler et al. 1989). Furthermore, the C/O ratio in S stars is intermediate between that of normal M giants (~ 0.2) and that of carbon stars (> 1). S stars were therefore traditionally considered as transition objects between normal M giants and carbon stars on the asymptotic giant branch (AGB) (e.g., Iben & Renzini 1983). Internal nucleosynthesis processes related to the thermal pulses (a recurrent thermal instability affecting the He-burning shell in AGB stars) could possibly produce the s-process elements (see the discussion by Sackmann & Boothroyd 1991), and the 'third dredge-up' (the descent of the lower boundary of the convective envelope into the region formerly processed by the thermal pulse) could bring them to the surface. The simple M–S–C evolution sequence faces, however, several problems, as discussed by e.g. Lloyd Evans (1984), Mould & Aaronson (1986) and Willems & de Jong (1986). The observation of Tc lines (an element with no stable isotopes) in some but not all S stars (Merrill 1952; Little et al. 1987) raised another major problem. If the s-process really occurred during recent thermal pulses in S stars, Mathews et al. (1986) predicted that Tc should be observed at the surface along with the other s-process elements.

A breakthrough in our understanding of the evolutionary status of S stars came with the realization that Tc-poor S stars are all members of binary systems (Brown et al. 1990; Jorissen et al. 1993; Johnson et al. 1993), and are likely the cooler analogues of the barium stars, a family of peculiar G–K giants first identified by Bidelman & Keenan (1951). Barium stars and S stars share the same abundance peculiarities (e.g., McClure 1984) and high rate of binaries with suspected white dwarf (WD) companions (Böhm-Vitense et al. 1984; McClure & Woodsworth 1990; Jorissen et al. 1997a). Both families are believed to owe their chemical peculiarities to the transfer of s-process-rich matter from the former AGB star (the progenitor of the current WD) to the (main sequence) progenitor of the current chemically-peculiar red giant.

It is therefore currently believed that two very different kinds of stars are found among S stars: Tc-rich *intrinsic* S stars that

Send offprint requests to: S. Van Eck
(e-mail: svaneck@astro.ulb.ac.be)

⋆ Based on data from the HIPPARCOS astrometry satellite

owe their chemical peculiarities to internal nucleosynthesis processes occurring during thermal pulses on the AGB, and Tc-poor *extrinsic* S stars, all members of binary systems with mass transfer responsible for the pollution of the S star envelope. Contrarily to intrinsic S stars that need to be thermally-pulsing AGB (TP-AGB) stars, extrinsic S stars may populate the first-ascent red giant branch (RGB), prior to the core He flash, or the early AGB (E-AGB) preceding the TP-AGB, since the mass-transfer scenario does not set any constraint on the *current* evolutionary stage of the extrinsic S star. A direct check of these predictions has been hampered till now by the difficulty in evaluating the absolute magnitude of S stars. Methods used so far include individual parallaxes (χ Cyg: Stein 1991), membership in a binary system with a detected main sequence companion (π^1 Gru: Feast 1953; 57 Peg: Hackos & Peery 1968; T Sgr: Culver & Ianna 1975), membership in a moving group (π^1 Gru, R Hya: Eggen 1972a; R And, HR 363, o^1 Ori: Eggen 1972b), membership in a cluster or association (WY Cas: Mavridis 1960; TT9, TT12: Feast et al. 1976), CaII K-line emission width (HD 191630, 57 Peg: Warner 1965; o^1 Ori: Boesgaard 1969). Most of these individual estimates were used by Scalo (1976) to locate S stars in the Hertzsprung-Russell (HR) diagram, with the conclusion that they fall above the luminosity threshold for TP-AGB stars, as derived from the early AGB model calculations available to Scalo. Although Scalo's conclusion appears to support the customary M-S-C sequence, statistical estimates based on the kinematics or space distribution of S stars pointed out a systematic difference between the average luminosity of non- or weakly-variable S stars and of Mira S stars, the latter being about 3 visual magnitudes brighter than the former (Takayanagi 1960; Yorka & Wing 1979). Such a segregation apparent in these early studies might already hint at the current dichotomy between extrinsic and intrinsic S stars.

The rather heterogeneous set of former luminosity determinations for S stars, along with our revised understanding of their evolutionary status, prompted the present study, based on the trigonometrical parallaxes provided by the HIPPARCOS satellite. Its aim is to locate both kinds of S stars in the HR diagram, and to compare their respective locations with stellar evolutionary tracks.

Our HIPPARCOS sample of S stars is described in Sect. 2. The method used for deriving their bolometric magnitudes is detailed in Sect. 3. The HR diagram of S stars is discussed in Sect. 4, with special emphasis on the comparison with theoretical evolutionary tracks and with S and C stars in the Magellanic Clouds. Finally, the correlation between the infrared colours of S stars and their location on the giant branches is discussed in Sect. 5.

2. S stars in the HIPPARCOS catalogue

A full discussion of the HIPPARCOS mission can be found in the HIPPARCOS catalogue (ESA 1997). Cross-identifications between the HIPPARCOS catalogue and the *General Catalogue of Galactic S Stars* (Stephenson 1984; GCGSS) yield 63 stars in common between the two catalogues. Of these, 22 are part of the HIPPARCOS general survey (a systematic monitoring of all stars down to magnitudes 7.3 – 9, depending on galactic latitude and spectral type), and 41 belong to samples included in the HIPPARCOS Input Catalogue (Turon et al. 1992abc) for a particular purpose. The sample of S stars studied in this paper can thus in no way be considered as a complete sample, since it rather reflects the particular interests prevailing at the time of construction of the HIPPARCOS Input Catalogue. A comparison with the GCGSS indicates that the HIPPARCOS sample of S stars is nevertheless complete down to V = 7.5.

Table 1 lists various identifications of the S stars considered in this paper. The different columns contain the following data:
1. HIPPARCOS Input Catalogue (HIC) number;
2-3. GCGSS and HD numbers;
4. variable name in the the *General Catalogue of Variable Stars* (Kholopov et al. 1985; GCVS);
5. variability type from the GCVS;
6. spectral type from the GCGSS;
7. presence (y) or absence (n) of technetium lines (from Little et al. 1987, Smith & Lambert 1988, from the compilation of Jorissen et al. 1993, or from Van Eck & Jorissen (in preparation) in the case of HIC 28297);
8-9. annual parallax π and its standard error σ_π (both expressed in milliarcseconds).

Table 2 lists the basic photometric properties of the S stars in the HIPPARCOS sample. The various columns contain the following data:
1. HIC number;
2-3. median Hp magnitude and its standard error $\sigma_{\rm Hp}$;
4. colour excess $E_{\rm B-V}$;
5. Johnson $V_{\rm J}$ magnitude from the HIPPARCOS catalogue;
6. dereddened $(V-K)_0$ colour index;
7. dereddened K_0 magnitude;
8. bolometric correction $BC_{\rm K}$ to the K magnitude;
9. bolometric magnitude $M_{\rm bol}$ (see Sect. 3 for details about the derivation of the quantities listed in columns 4–9);
10. method used for deriving the bolometric correction: (1) by integrating under the energy curve, or (2) from the $(BC_{\rm K}, V-K)$ relation of Bessell & Wood (1984);
11. source for the HIPPARCOS $(V-I)_{\rm C}$ colour [A-G: from $VRI_{\rm C}$ photometry; H-K: from $UBV_{\rm J}$ photometry; L-P: from HIPPARCOS and Star Mapper photometry; Q: specific treatment applied to long-period variables; R: from spectral type; see the HIPPARCOS and Tycho Catalogues (ESA 1997, Vol. 1, *Introduction and Guide to the Data*) for details];
12. duplicity flag (field H59 of the HIPPARCOS catalogue; see Sect. 4.1);
13. other identifications ('Hen' refers to the survey of S stars by Henize 1960).

One star (HIC 42650 = GCGSS 544) appears outlying in many respects. With the largest parallax in the sample and the second faintest Hp magnitude, it is intrinsically much fainter than all the other stars in the sample. It is also somewhat bluer, with $(B-V)_J$ = 1.39 and $(V-I)_C$ = 1.65, compared to average colour indices of $\langle(B-V)_J\rangle$ = 1.79 and $\langle(V-I)_C\rangle$ = 2.72 for the whole sample. A low-resolution spectrum ($\Delta\lambda \sim 0.3$

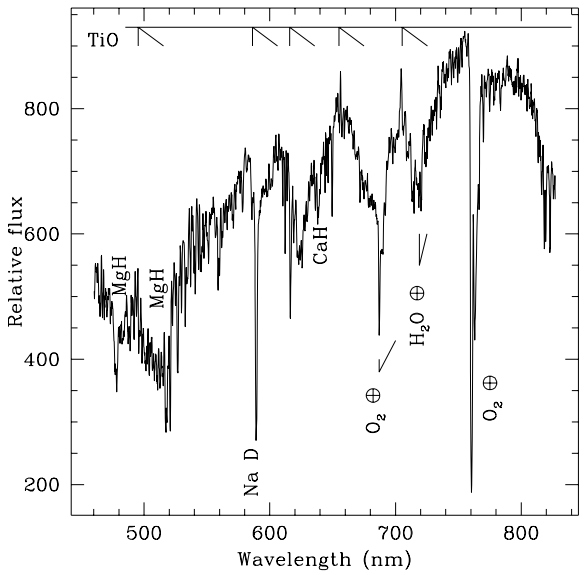

Fig. 1. The spectrum of HIC 42650 = GCGSS 544, with the principal spectral features identified

nm) of this star, covering the spectral range 440 – 820 nm, has been obtained at the *European Southern Observatory* (ESO, La Silla, Chile) on the 1.52-m telescope equipped with the Boller & Chivens spectrograph (grating #23 + filter GG 420; 114 Å mm^{-1}) and a Loral/Lesser thinned, UV-flooded 2048x2048 CCD (CCD#39; 15 μm pixels). The flux response curve of the system has been calibrated using the spectrophotometric standard star LTT 4816.

The spectrum of GCGSS 544 appears to be that of a M0-M1 dwarf, as can be seen on Fig. 1 from the strong MgH (λ478.0 and λ521.1) and CaH (λ638.2 and λ638.9) bands, as well as from the strong Na D line superimposed on moderately strong TiO bands (Jaschek & Jaschek 1987). This classification is consistent with its absolute visual magnitude $M_{\rm v}$= 8.6 derived from its HIPPARCOS parallax and V_J magnitude. That star is thus misclassified as S star, since there is no trace whatsoever of ZrO bands in its spectrum.

The case of T Cet (= HIC 1728) is also conflicting, since it was classified as M5-6Se in the original paper by Keenan (1954) defining the S class, and reclassified as M5-6Ib-II in the Michigan Spectral Survey (Houk & Cowley 1975). The spectra of supergiants and weak S-type stars look very similar at the low plate dispersions used in classification work, and are therefore easily confused (e.g., Lloyd Evans & Catchpole 1989). T Cet has nevertheless been kept in our final list until higher resolution spectra resolve these equivocal classifications.

The star HIC 27066 (= GCGSS 157) has HIPPARCOS colours that do not match those of an S star [$(B-V)_J$ = 0.80 and $(V-I)_C$ = 0.83]. HIPPARCOS found it to be a close visual binary with a separation of 0.262 arcsec, the companion being 1.55 mag fainter in the Hp band. The colour indices measured by HIPPARCOS correspond to the composite light from the system.

The only other S star found by HIPPARCOS to be a close visual binary (with an angular separation of 0.18 arcsec) is HIC 19853. Although its colour indices are not atypical for a late-type star, the measured colours must clearly be composite since the companion is only 0.35 mag fainter in the Hp band.

These two stars have been excluded from our final sample. Among the 60 remaining S stars, 21 do exhibit technetium lines in their spectrum, 22 do not, and the Tc content is unknown for the remaining 17 stars.

The only trigonometrical parallax for an S star with a small relative error available in the literature prior to the HIPPARCOS mission is that obtained by Stein (1991) for the Mira S star χ Cyg. His value (8.8 $\pm$ 1.9 mas) is in good agreement with the HIPPARCOS parallax listed in Table 1.

3. Colours and bolometric magnitudes

3.1. Colours

Although the $(B-V)_{\rm J}$ and $(V-I)_{\rm C}$ (where the subscripts J and C stand for the Johnson and Cousins photometric systems, respectively) colour indices are directly provided by the HIPPARCOS catalogue, we felt that the $(V-K)_{\rm J}$ colour index, derived on a case-by-case basis, is a more appropriate temperature indicator. For most of the stars in our sample, the $(V-I)_{\rm C}$ index listed in the HIPPARCOS catalogue has been derived from a fiducial relation $(V-I)_{\rm C}$= $f(B-V)_{\rm J}$ calibrated on normal M giants (as indicated by the flags H-P in column $S_{\rm V-I}$ of Table 2). Several S stars in our sample, however, fall outside the validity range of such a calibration, so that $(V-I)_{\rm C}$ as provided by the HIPPARCOS catalogue is not a reliable temperature indicator for our purpose.

As discussed by Ridgway et al. (1980), $B-V$ for late-type stars is not a good temperature indicator either, because the temperature has opposite effects on $B-V$: when the temperature decreases, the absorption in the V band due to TiO bands increases (thus decreasing $B-V$), whereas the black body continuum tends to increase the $B-V$ index. By contrast, these two effects act together to increase $V-K$.

The $V-K$ index has therefore been constructed from individual K magnitudes collected from the literature, mostly from the *Two-Micron Sky Survey* (Neugebauer & Leighton 1969; TMSS), but also from Wing & Yorka (1977), Catchpole et al. (1979), Chen et al. (1988), Noguchi et al. (1991) and Fouqué et al. (1992); it is available for 46 stars as listed in Table 2. The adopted V magnitude corresponds to the $V_{\rm J}$ magnitude listed in the HIPPARCOS catalogue. It has been obtained by the HIPPARCOS reduction consortia from a $(H_{\rm p}-V_{\rm J}, (V-I)_{\rm C})$ relation, with $(V-I)_{\rm C}$ derived by different methods as listed in column $S_{\rm V-I}$ of Table 2. According to the HIPPARCOS reduction consortia (ESA 1997, Vol. 1, *Introduction and Guide to the Data*), that relation is quite well defined from classical photometry in the range $-0.4 < (V-I)_{\rm C} < 3.0$ (which holds for 47 S stars), with uncertainties of less than 0.01 mag. The red extension down to $(V-I)_{\rm C}$= 5.4 (15 S stars) was defined using observations of Mira variables devoted to that purpose, resulting in an un-

Table 1. S stars in the HIPPARCOS catalogue: Identifications and parallaxes

HIC	GCGSS	HD	Var	Var type	Sp.	Tc	π	σ_π
621	3	310			S3,1	n	2.50	0.69
1728	8	1760	T Cet	SRc	M5-6Se; M5-6Ib-II	y	4.21	0.84
1901	9	1967	R And	M	S5-7/4-5e	y	-0.06	6.49
5091	22	6409			M2wkS	n	2.43	0.89
5772	26	7351			S3/2	n	3.21	0.82
8876	45				S3/1	n	-1.92	1.50
10687	49	14028	W And	M	S7/1e	y	-1.17	3.17
17296	79	22649	BD Cam	Lb	S4/2	n	6.27	0.63
21688	104	29704			S:	n	1.84	1.00
22667	114	30959	o^1 Ori	SRb	S3/1	y	6.02	0.94
25092	133	35155			S4,1	n	1.32	0.99
26718	149	37536	NO Aur	Lc	M2S	y	2.38	0.97
28297	178	40706			S2,1	n	1.17	0.88
30301	212	44544	FU Mon	SR	S7/7 (SC)		0.30	1.58
32627	260	49368	V613 Mon	SRb:	S3/2	n	1.65	1.11
32671	265	49683			M4S		-0.18	1.07
33824	283	51610	R Lyn	M	S5/5e		-3.39	1.79
34356	307	53791	R Gem	M	S4*1	y	-6.22	6.50
35045	312	54587	AA Cam	Lb	M5S	y	1.24	1.02
36288	347	58521	Y Lyn	SRc	M6S	y	4.03	1.33
37521	382	61913	NZ Gem	SR	M3S	n?	3.19	0.79
38217	411	63733			S4/3	y?	0.00	0.99
38502	422	64332	NQ Pup	Lb	S5/2	y	3.01	1.11
38772	436		SU Pup	M	S4,2		-1.75	1.81
40977	494	70276	V Cnc	M	S3/6e		26.58	42.74
45058	589	78712	RS Cnc	SRc:	M6S	y	8.21	0.98
54396	722	96360			M3	n	2.10	0.90
59844	788		BH Cru	M	S5,8e (SC)		1.64	0.99
62126	803	110813	S UMa	M	S3/6e	y	0.63	0.94
64613	815				S3,3		-1.90	2.99
64778	816	115236	UY Cen	SR	S6/8 (CS)		1.66	1.04
66783	826	118685			S6,2	n	3.42	0.65
67070	829				M1wkS	n	2.27	1.06
68837			U Cir	SR	C		-1.92	1.51
71348	804	110994	BQ Oct	Lb:	S5,1		2.08	0.57
72989	867	131217			S6,2	n	4.24	1.02
77619	903	142143	ST Her	SRb	M6.5S	y	3.22	0.75
81970	937				M2S	n	3.32	1.14
82038	938	151011			Swk	n	4.30	1.07
87850		163990	OP Her	SRb	M6S	y	3.26	0.54
88620	1014	164392					2.09	1.06
88940	1023	165774			S4,6	n	0.23	1.50
89316	1025	165843			S2,1		1.47	1.05
90723	1053	170970			S3/1	y	1.83	0.67
94706	1117	180196	T Sgr	M	S5/6e	y	-31.67	9.28
97629	1165	187796	χ Cyg	M	S7/1.5e	y	9.43	1.36
98856	1188	190629	AA Cyg	SRb	S6/3	y	0.86	0.88
99124	1192	191226			M1S-M3SIIIa	n	0.39	0.71
99312	1194	191589			S:	n	2.25	0.77
99758	1195	191630			S4,4	y	1.18	0.81
100599	1211		V865 Aql	M	S7,2		-1.28	1.91
101270	1224	195665	AD Cyg	Lb	S5/5		-0.96	1.15
103476	1254	199799			MS		2.16	0.82
110146	1292	211610	X Aqr	M	S6,3e:		-4.01	5.73
110478	1294	212087	π^1 Gru	SRb	S5,7:	y	6.54	1.01
112227	1304	215336			Swk	n	0.74	0.92
112784	1309		SX Peg	M	S3/6e		2.12	2.99
113131	1315	216672	HR Peg	SRb	S4/1	y	3.37	0.94
114347	1322	218634	57 Peg	SRa	M4S	n	4.28	0.88
115965	1334				S2/3:	n	1.72	1.26
HIPPARCOS close visual binaries								
19853	89	26816			S	y	3.79	1.05
27066	157				S		1.13	3.50
Misclassified S star								
42650	544				MS[a]		32.13	1.50
Comparison barium star								
68023		121447			K7IIIBa5; S0	n[b]	428±71 pc [c]	

Remarks:
a: HIC 42650 is an early M dwarf rather than a MS star
b: Little et al. (1987)
c: Distance derived by Mennessier et al. (1997) from a maximum-likelihood estimator based on the HIPPARCOS parallax

Table 2. S stars in the HIPPARCOS catalogue: Photometry

HIC	Hp	$\sigma_{\rm Hp}$	$E_{\rm B-V}$	$V_{\rm J}$	$(V-K)_0$	K_0	$BC_{\rm K}$	$M_{\rm bol}$		$S_{\rm V-I}$	Dupl	Other ident.
621	7.570	0.003	0.000	7.50	4.38	3.12	2.74	-2.14	2	O		Hen 1
1728	5.439	0.033	0.000	5.61	6.5	-0.89	2.91	-4.85	1	O		
1901	10.705	0.011		10.71		-0.11				K	V	
5091	7.462	0.004	0.042	7.44	5.04	2.27	2.84	-2.95	2	O		
5772	6.395	0.004	0.049	6.33	4.65	1.53	2.68	-3.25	1	F		HR 363
8876	9.072	0.002		8.97						L		+21°255
10687	8.075	0.226		8.60		0.7				O		
17296	5.095	0.003	0.041	5.06	4.78	0.15	2.77	-3.09	1	C	O	HR 1105
21688	8.225	0.009	0.000	8.23	5.64	2.59	2.91	-3.16	2	O		Hen 3
22667	4.702	0.005	0.121	4.71	4.96	-0.62	2.85	-3.87	1	O	V	
25092	6.882	0.011	0.128	6.82	4.46	1.97	2.76	-4.66	2	F		
26718	6.243	0.011	0.245	6.23	4.67	0.8	2.74	-4.57	1	C		
28297	8.987	0.002	0.029	8.88						L		Hen 7
30301	8.520	0.032	0.327	9.76	7.35	1.4	3.03		1	O		
32627	7.749	0.004	0.051	7.73	4.93	2.64	2.83	-3.43	2	O		
32671	8.232	0.006		8.38		2.07				O		
33824	9.922	0.029		9.93		1.91				K		
34356	7.529	0.456		7.53		2.12				P	V	
35045	7.578	0.007	0.039	7.69	6.01	1.56	2.95	-5.01	2	O	V	
36288	6.897	0.005	0.058	7.27	7.63	-0.54	3.08	-4.43	1	O	V	
37521	5.587	0.003	0.027	5.55	4.85	0.61	2.86	-4.01	1	G		HR 2967
38217	7.981	0.002		7.90						F		
38502	7.532	0.015	0.072	7.52	5.17	2.13	2.86	-2.61	2	F	V	
38772	9.609	0.218		9.64		2.64				K		Hen 32
40977	9.262	0.152	0.004	9.25						K	X	
45058	5.450	0.026	0.002	6.04	7.74	-1.71	3.07	-4.06	1	O		
54396	8.075	0.006	0.000	8.05						O		
59844	7.737	0.118	0.163	7.74						K		Hen 120
62126	8.909	0.148	0.000	8.94	5.95	2.99	2.87		1	K		
64613	11.404	0.021		11.33		2.85				K		Hen 134, -30°10427
64778	6.787	0.033	0.088	6.85	6.09	0.49	2.85	-5.55	1	L	V	Hen 135
66783	6.832	0.007	0.062	6.91	5.82	0.9	2.93	-3.49	2	O		Hen 138
67070	8.541	0.002	0.009	8.43						L		-2°3726
68837	9.609	0.013		9.54						J	V	C* 2142
71348	6.806	0.005	0.106	6.82	5.16	1.33	2.86	-4.21	2	O		Hen 127
72989	7.425	0.004	0.204	7.45						O		Hen 150
77619	6.920	0.026	0.000	7.69	8.55	-0.86	3.11	-5.20	2	O		
81970	7.803	0.004	0.173	7.99	5.63	1.83	2.91	-2.64	2	O		−13°4495
82038	6.689	0.002	0.190	6.60	4.59	1.43	2.78	-2.62	2	L		
87850	6.105	0.010	0.022	6.22	6.09	0.06	2.92	-4.45	1	O		
88620	8.448	0.004	0.072	8.39						O		Hen 183
88940	8.211	0.003	0.186	8.17						O		Hen 186
89316	8.412	0.005	0.082	8.37						O		Hen 187
90723	7.457	0.002	0.041	7.42	4.88	2.41	2.82	-3.45	2	O		
94706	10.826	0.223		10.78		1.05	3.14		1	K	V	
97629	6.169	0.168	0.004	7.91	7.69	-1.73	3.27	-3.58	1	O	V	
98856	8.159	0.037	0.491	8.16	6.26	0.39	2.94		1	K		
99124	7.374	0.002	0.491	7.28	3.4	2.37	2.52		2	L		
99312	7.368	0.001	0.081	7.26						H		
99758	6.757	0.004	0.029	6.74	5.05	1.6	2.71	-5.33	1	O		Hen 197
100599	9.642	0.134		10.34		1.49				Q		+0°4492
101270	8.607	0.011		8.61		1.18				K		
103476	7.248	0.016	0.071	7.36	5.99	1.15	2.95	-4.22	2	O		
110146	10.188	0.179		10.82		2.9				Q	V	
110478	5.495	0.011	0.000	6.42	8.55	-2.13	3.12	-4.93	1	O	V	Hen 202
112227	7.929	0.001	0.089	7.82						L		
112784	9.241	0.176	0.056	9.25						K	V	
113131	6.346	0.016	0.050	6.39	5.47	0.77	2.86	-3.73	1	O	V	HR 8714
114347	5.033	0.011	0.024	5.05	5.47	-0.5	3	-4.34	1	F		
115965	9.536	0.003	0.056	9.43						K		+28°4592
HIPPARCOS close visual binaries												
19853	7.607	0.010	0.120	7.90						O	C	+23°654
27066	11.274	0.010	0.327	11.12						R	C	
Misclassified S star												
42650	11.118	0.005	0.009	11.03						I		
Comparison barium star												
68023			0.056		3.78	4.090	2.69	-1.40	1			

certainty of 0.03–0.05 mag. For indices down to $(V-I)_{\rm C}$= 9.0 [only χ Cyg is concerned, with $(V-I)_{\rm C}$= 6.1], the HIPPARCOS reduction consortia adopted a linear extrapolation of the previous relation. To avoid the uncertainties inherent to such an extrapolation, a (flux) average of the numerous $V_{\rm J}$ measurements of χ Cyg available in the literature has been preferred over the linear extrapolation.

In summary, the uncertainty on $V_{\rm J}$ introduced by the colour transformation applied on Hp is largely offset by the fact that the Hp magnitude is a good time average over a uniform period of time (the duration of the HIPPARCOS mission), the same for all the stars. As discussed in Sect. 4.1, the intrinsic variability of S stars is indeed a major source of uncertainty on their location in the HR diagram.

3.2. Bolometric magnitudes

Since most of the flux from S stars is radiated in the near-infrared, the bolometric correction is best determined from near-infrared magnitudes. Moreover, the near-infrared and bolometric variability is much smaller than the visual amplitude of variations (Mira-type variables which vary typically by 6 to 8 mag in the visual region, vary by less than 1 mag in the K band; Feast et al. 1982). Therefore, the bolometric correction $BC_{\rm K}$ in the K band (defined as $M_{\rm bol}$ = K + $BC_{\rm K}$) has been adopted in this work (and listed in Table 2).

In order to compute bolometric corrections, an extensive set of magnitudes ranging from the ultraviolet to the far IR has been collected from the literature. This set includes Johnson $UBVRIJHKLM$ magnitudes when available, as well as good quality fluxes at 4.2, 11.0, 19.8 and 27.4 μm from the Revised Air Force Four-Color Infrared Sky Survey (Price & Murdock 1983), and four-colour infrared photometry from Gillett & Merrill (1971). The IRAS 12, 25, 60 and 100 μm fluxes (with a quality flag 3) from the second edition of the *Point Source Catalogue* (IRAS Science Team 1988) were also used, or when available, the reprocessed IRAS fluxes provided by Jorissen & Knapp (1997). When several measurements in the same filter are available, a flux average has been computed.

All magnitudes bluer than 4.8μm have been corrected for interstellar reddening and absorption, using the extinction law as provided by Cohen et al. (1981) for the $BVRIHKL$ filters and by Koornneef (1983) for the J and M filters. The visual extinction $A_{\rm V}$ was derived either from Neckel & Klare (1980) with the distance derived from the HIPPARCOS parallax, or from Burstein & Heiles (1982) for stars with galactic latitudes $|b| > 10^\circ$. In the latter case, the $E_{\rm B-V}$ value provided by Burstein & Heiles (1982) was reduced by the factor $[1-\exp(-10d\sin|b|)]$, where d stands for the distance in kpc. In the remaining cases, the cosecant formula (Feast et al. 1990) $E_{\rm B-V}$ = 0.032 (cosec$|b|-1$) $[1-\exp(-10\,d\sin|b|)]$ was used. The adopted $E_{\rm B-V}$ values are listed in Table 2.

The deredenned $BVRIJKLM$ magnitudes have then been converted into fluxes using the zero-magnitude fluxes provided by Johnson (1966). This particular choice will be justified below. The zero-magnitude flux in the H band was taken from Jaschek (1978) and, for the remaining bands, from the original papers quoted above.

A limited sample of 17 stars have enough broad-band colours available ($BVRIJHK$, as well as IRAS 12, 25 and 60 μm) to derive the bolometric magnitude by a direct integration of the available fluxes over wavelength. More precisely, the trapezoidal rule has been used on the curve λF_λ versus $\log\lambda$. The zero point of the bolometric magnitude has been defined from the requirement that L = 3.86 10^{33} erg s^{-1} corresponds to $M_{\rm bol}$ = 4.75 for the Sun.

If the available photometric data was too scarce to derive the bolometric magnitude from a direct integration, it has been derived instead from the $(BC_{\rm K}, V-K)$ relation of Bessell & Wood (1984) applicable to oxygen-rich stars. For the 17 S stars where both methods are applicable, they yield consistent results (with a r.m.s. deviation of 0.1 mag), provided that the zero-magnitude fluxes of Johnson (1966) be adopted (as was done by Bessell & Wood 1984). If the zero-magnitude fluxes listed by Jaschek (1978) are used instead, somewhat lower bolometric corrections $BC_{\rm K}$ (i.e. brighter bolometric magnitudes, by about 0.06 mag) are obtained.

A bolometric magnitude $M_{\rm bol}$ = -3.74, based on the same HIPPARCOS parallax, has recently been derived by van Leeuwen et al. (1997) for χ Cyg, and agrees well with our value -3.58 listed in Table 2.

4. The HR diagram of S stars

The $V-K$ colours and the bolometric magnitudes derived as discussed in Sect. 3, combined with the HIPPARCOS parallaxes, provide the HR diagram of S stars presented in Fig. 2. Only the 30 S stars with an available K magnitude and with $0 < \sigma_\pi/\pi < 0.85$ (see Fig. 3) have been plotted. Despite the sometimes large uncertainties affecting $V-K$ or $M_{\rm bol}$ (as discussed in Sect. 4.1 below), a segregation between extrinsic and intrinsic S stars is readily apparent, with *extrinsic S stars being intrinsically fainter and bluer than intrinsic S stars*.

4.1. Uncertainties on the HR diagram

The two major sources of uncertainty on the position of an S star in the HR diagram are the stellar intrinsic variability and the error on the parallax π.

The intrinsic variability of S stars has an impact on both $V-K$ and $M_{\rm bol}$. The variability in the V band and, to a lesser extent, in the K band, leads to a variation of $V-K$, and thus of $BC_{\rm K}$ (Sect. 3.2). If $BC_{\rm K}$ was derived from simultaneous V and K measurements, it could be expected that the variations in K and in $BC_{\rm K}$ would cancel to a large extent, thus leaving only a moderate variation in $M_{\rm bol}$. However, since the V and K data used in this study do not result from simultaneous observations, the expected cancellation will not occur. Its impact on $M_{\rm bol}$ is, however, difficult to evaluate. It seems nevertheless unlikely that this effect could lead to a systematic upwards shift of all intrinsic S stars that would be responsible for the observed segregation between intrinsic and extrinsic S stars. The impact of

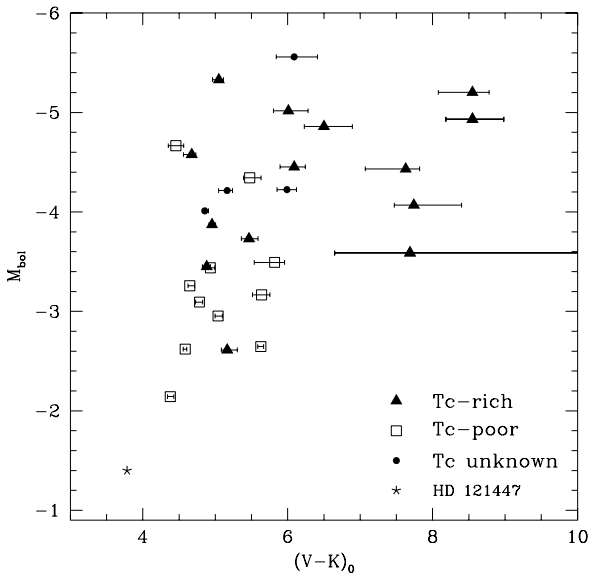

Fig. 2. The HR diagram for S stars with $0 < \sigma_\pi/\pi < 0.85$. Filled triangles correspond to Tc-rich S stars, open squares to Tc-poor S stars and dots to S stars with unknown Tc. HD 121447, the boundary case between Ba and S stars (see Sect. 4.2), is represented by $\star$. The error bar provides the uncertainty on $V-K$ caused by the intrinsic variability of the HIPPARCOS Hp magnitude; it covers the range in Hp between the 5th and 95th percentiles

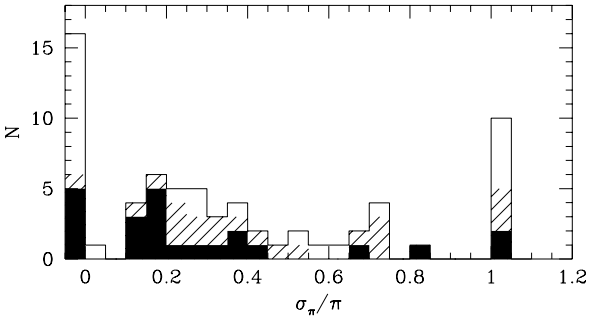

Fig. 3. Distribution of the relative error σ_π/π on HIPPARCOS parallaxes π for S stars. The hatched and black parts of the histogram correspond to Tc-poor and Tc-rich S stars, respectively. Stars with negative parallaxes and stars with $\sigma_\pi/\pi > 0.85$ have been assigned to the leftmost and rightmost bins, respectively

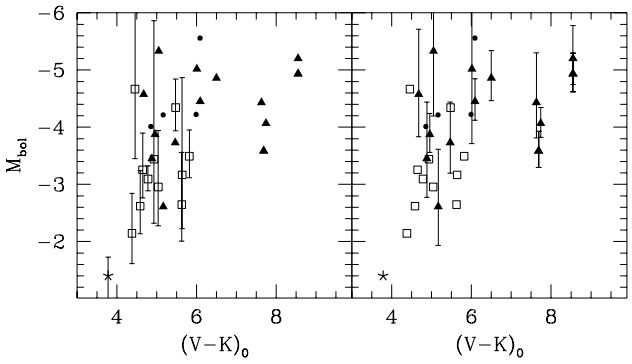

Fig. 4. The uncertainty on $M_{\rm bol}$ due to the uncertainty σ_π on the parallax π. The error bar extends from $M_{\rm bol}(\pi+\sigma_\pi)$ to $M_{\rm bol}(\pi-\sigma_\pi)$. Left panel: parallactic errors for Tc-poor S stars; right panel: parallactic errors for Tc-rich S stars. Symbols are as in Fig. 2

the intrinsic variability on $V-K$ is easier to estimate. Its effect is shown on Fig. 2 from the variation recorded in the Hp magnitude over the $\sim$ 1230 d duration of the HIPPARCOS mission. The smaller variation due to K has not been taken into account. Clearly, the uncertainty on $V-K$ due to the intrinsic variability does not jeopardize the observed segregation between extrinsic and intrinsic S stars. An interesting by-product of Fig. 2 is the increase of the amplitude of variations towards cooler and more luminous stars (see also Eyer & Grenon 1997 and Jorissen et al. 1997b).

The impact on the bolometric magnitude of the uncertainty on the parallax is shown in Fig. 4, presenting (separately for intrinsic and extrinsic S stars) the range of $M_{\rm bol}$ corresponding to $\pi \pm \sigma_\pi$ (see Arenou et al. 1995 and Lindegren 1995 for a discussion of the external errors of HIPPARCOS parallaxes and of the accuracy of the zero-point). As discussed by van Leeuwen et al. (1997), there is a specific error source on the parallax for nearby Mira variables, as some of these stars were found to have asymmetrical spatial light distributions. Changes in these asymmetries might affect the derived parallax. The flag 'V' in field H59 of the HIPPARCOS catalogue possibly reflects such effects, as it refers to a 'variability-induced mover'. This flag is set for 14 stars in our sample, mostly nearby Miras (see column 'Dupl' in Table 2). Like van Leeuwen et al. (1997), we assume that any such effect will add only additional random scatter to the mean results.

Part of the overlap in luminosity between extrinsic and intrinsic S stars in the HR diagram may actually be attributed to the large error bars of the interloping stars (NQ Pup and HD 170970[1] among intrinsic S stars, and HD 35155 among the extrinsic S stars). That explanation does not hold true, however, for the high-luminosity, Tc-poor S star 57 Peg ($M_{\rm bol} = -4.3$), which has a small uncertainty on its parallax ($\sigma_\pi/\pi = 0.21$). That star is special in many respects, since it has an A6V companion instead of the WD companion expected for extrinsic S stars in the framework of the binary paradigm (Sect. 1). It is further discussed in Appendix A.

The case of HD 35155 deserves further comments. This extrinsic S star has the second largest relative error on the parallax. It is a binary system with an orbital period of 642 $\pm$ 3 d in a nearly circular orbit (Jorissen & Mayor 1992), yielding an orbital separation of about 2 AU assuming typical masses of 1.6 and 0.6 $M_\odot$ for the S star and its suspected white dwarf companion (see Jorissen et al. 1997a). The corresponding angular separation on the sky (a) will thus be about twice the annual

[1] The presence of Tc in HD 170970 is somewhat uncertain, though, since the central wavelength of the blend containing the λ426.2 Tc line lies at the very boundary between Tc-rich and Tc-poor stars (Smith & Lambert 1988)

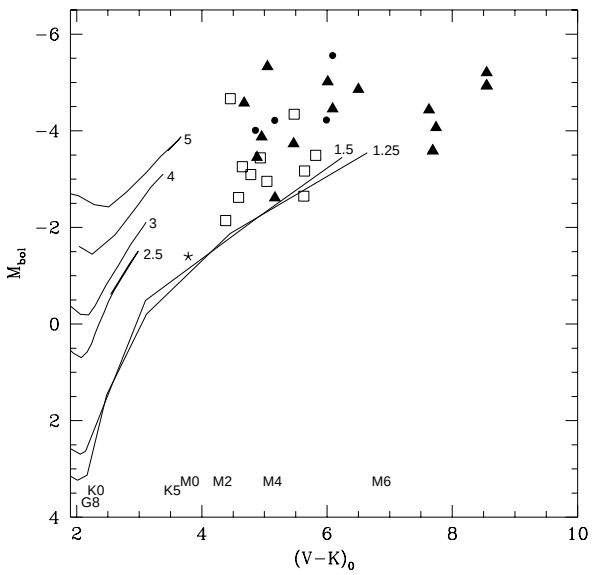

Fig. 5. The location of the RGB (up to the onset of core He-burning) for stars of various masses (as labelled, in $M_\odot$) and metallicity $Y = 0.3$, $Z = 0.02$, according to Schaller et al. (1992). The ($V - K$, spectral types) calibration is from Ridgway et al. (1980). Other symbols are as in Fig. 2

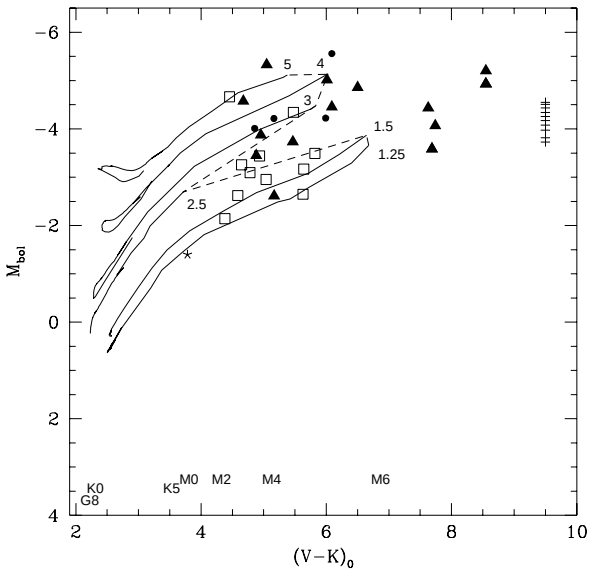

Fig. 6. Same as Fig. 5, but for the early AGB up to the first thermal pulse (Charbonnel et al. 1996). To guide the eye, a dashed line connects the starting point of the TP-AGB on the various tracks. The crosses along the right-hand axis provide the luminosities of the first ten thermal pulses in a 1.5 $M_\odot$, $Z = 0.008$ star (corresponding to the LMC metallicity) computed by Wagenhuber & Tuchman (1996). Other symbols are as in Fig. 2

parallax (since $a = A\pi$, where A is the orbital separation expressed in AU). There is no indication whatsoever that the orbital motion of HD 35155 has been detected by HIPPARCOS. However, since the orbital period is of the order of the duration of the HIPPARCOS mission and the parallax is small (1.32 ± 0.99 mas), this system represented a difficult challenge for the reduction consortia. The orbital motion has in fact been detected (flag 'O' in column 'Dupl' of Table 2) for another short-period S star (HIC 17296 = HD 22649; P = 596 d), but the situation is more favourable in this case, because of its larger parallax (π = 6.27 mas compared to π = 1.32 mas for HD 35155).

Finally, one should be aware that the observed distribution of absolute magnitudes of a sample of stars may be altered by various statistical biases, depending on the selection criteria of the sample (e.g. Brown et al. 1997; Luri & Arenou 1997). Monte-Carlo simulations in Appendix B show that the observed segregation between extrinsic and intrinsic S stars cannot plausibly result from statistical biases altering the true absolute-magnitude distributions.

4.2. Comparison with theoretical RGB and AGB evolutionary tracks

Fig. 5 compares the position of S stars in the HR diagram with the RGB (i.e. up to the onset of core He-burning) for stars of different masses and of metallicity $Y = 0.3$, $Z = 0.02$ (Schaller et al. 1992). Fig. 6 is the same as Fig. 5, but for the E-AGB, up to the first thermal pulse (Charbonnel et al. 1996).

The effective temperatures of all these models have been converted to $V - K$ colours using the calibration of Ridgway et al. (1980) for class III giants, which is strictly valid only in the range $2.2 < V - K < 6.8$.

The predicted location of the giant branch in the HR diagram is known to depend sensitively upon model parameters like the convective mixing length or the atmospheric opacities. For the Geneva evolutionary tracks used here, these model parameters have been calibrated so as to reproduce the observed location of the red giant branches of more than 75 clusters (Schaller et al. 1992). The comparison of these tracks with the observed location of the S stars in the HR diagram is thus meaningful. The main result of the present study is apparent on Fig. 6: the line marking the onset of thermal pulses matches well the limit between intrinsic and extrinsic S stars, so that *Tc-rich intrinsic S stars may be associated with thermally-pulsing AGB stars* (the only possible exception being NQ Pup, but see the discussion about errors below).

The previous result provides interesting constraints on the occurrence of both the s-process and the third dredge-up in thermally-pulsing AGB stars, by suggesting that those processes operate from the very first thermal pulses on, a conclusion already reached by several authors (e.g., Richer 1981; Scalo & Miller 1981; Miller & Scalo 1982) from the luminosity distribution of carbon stars in the Magellanic Clouds (see, however, the discussion of Sect. 4.3). Because there is little change in luminosity from one pulse to the next (see Fig. 6), and because of the uncertainties affecting the location of individual S stars in the HR diagram, it is difficult, however, to set a limit on the exact number of pulses necessary to change a normal M giant into an (intrinsic) S star. Moreover, the statistical biases discussed in

Appendix B shift the lower boundary of the observed luminosity distribution of Tc-rich S stars *below* the true threshold. The Monte-Carlo simulations presented in Appendix B predict that the faintest star in the sample of 14 Tc-rich S stars displayed in Fig. 6 will be observed 0.7 to 1.5 mag below the lower boundary of the true luminosity distribution (see Fig. B1). This is well in line with the observed location of the Tc-rich S star NQ Pup (see Sect. 4.1) below the TP-AGB threshold luminosity.

As far as extrinsic S stars are concerned, the present data alone do not permit to distinguish between them populating the RGB or the E-AGB of low-mass stars. Neither does the mass-transfer scenario (Sect. 1) set any constraint on the *current* evolutionary stage of the extrinsic S star. However, when both the RGB and the E-AGB are possible, evolutionary time-scale considerations clearly favor the RGB over the AGB. Besides, the analysis of the orbital elements (Jorissen et al. 1997a) points towards them being low-mass stars, with an average mass of 1.6 ± 0.2 M$_\odot$. This value is in excellent agreement with their position in the HR diagram of Fig. 5 (two exceptions are HD 35155 and 57 Peg; see Sects. 4.1 and Appendix A).

Contrarily to what might be inferred from the smooth transition between intrinsic and extrinsic S stars in the HR diagram, the two kinds of S stars belong to distinct galactic populations, intrinsic S stars being more concentrated towards the galactic plane (Jorissen et al. 1993; Jorissen & Van Eck 1997; Van Eck & Jorissen, in preparation). Extrinsic and intrinsic S stars are thus not simply successive stages along the evolution of stars in the same mass range.

Note that the lower left boundary of the region occupied by extrinsic S stars is set by the condition that $T_{\rm eff}$ be low enough in order that ZrO bands may form. Such a threshold roughly corresponds to the transition between K and M giants (see the spectral types labelling Fig. 5), so that extrinsic S stars should merge into the KIII barium stars at lower luminosities and higher $T_{\rm eff}$ along the RGB (e.g., Jorissen et al. 1997a). As an example, the transition object HD 121447, classified either as K7IIIBa5 (Lü 1991) or S0 (Keenan 1950), has been located in Fig. 5 following the methods presented in Sect. 3, using the photometry obtained by Hakkila & McNamara (1987) and the HIPPARCOS distance provided by Mennessier et al. (1997).

4.3. Comparison with S and carbon stars in external systems

Several S stars have been found in the Magellanic Clouds and in a few other nearby galaxies, allowing a direct comparison of their luminosities with those of galactic S stars derived from the HIPPARCOS trigonometric parallaxes (Fig. 7):

- In a study of 90 long-period variables in the Magellanic Clouds, Wood et al. (1983) identified 14 MS stars (labelled as W83 on Fig. 7) in the range $-7 \leq M_{\rm bol} \leq -5$;
- In a magnitude-limited survey of several fields in the outer regions of the northern LMC, Reid & Mould (1985) identified 10 S stars (labelled as R85 on Fig. 7) in the range $-5.0 \leq M_{\rm bol} \leq -3.9$;
- In a sample extracted from the faint tail of the Westerlund et al. (1981) LMC survey of late-type giants, Lundgren (1988) finds 6 S stars (labelled as L88 on Fig. 7) in the range $-5.7 \leq M_{\rm bol} \leq -4.8$;
- Bessell et al. (1983) and Lloyd Evans (1983a, 1984) find 16 S stars (labelled as B83, L83 and L84 on Fig. 7, with bolometric magnitudes provided in Tables A1 and A2 of Westerlund et al. 1991) in LMC clusters with $-4.8 \leq M_{\rm bol} \leq -4.4$ (excluding NGC 1651/3304, quite far from the cluster center, possibly a field star, and the close pair LE1+2 in NGC 1987);
- S stars have also been found in other galaxies: for example, Aaronson et al. (1985) find one S star with $M_{\rm bol} = -5.15$ in NGC 6822, Brewer et al. (1996) discover one S star with $M_{\rm bol} = -5.3$ in M31, and Lundgren (1990) finds seven S stars in the range $-4.9 \leq M_{\rm bol} \leq -3.1$ in the Fornax dwarf elliptical galaxy (labelled as L90 on Fig. 7).

The bolometric-magnitude range for all these S stars in external systems has been plotted in Fig. 7. Their luminosities are generally comparable to those of the galactic Tc-rich S stars, with the exception of the brighter W83 S stars. These W83 S stars extend up to the theoretical AGB tip corresponding to the Chandrasekhar limit for the degenerate core. Smith et al. (1995) have shown that, in the Magellanic Clouds, these S stars with $-7 \leq M_{\rm bol} \leq -6$ are all Li- strong stars with $M \gtrsim 4$ M$_\odot$. In the solar neighbourhood, these Li-strong S stars are rare (Catchpole & Feast 1976; Lloyd Evans & Catchpole 1989). The only such star in the present HIPPARCOS sample is T Sgr, but its HIPPARCOS parallax is useless (Table 1).

Conversely, in all the external systems, there appears to be a lack of low-luminosity S stars with respect to the solar neighbourhood. In the Magellanic Cloud fields surveyed, this lack of low-luminosity S stars may clearly be attributed to the limited sensitivity of the surveys (see R85 and L88 in Fig. 7). The situation is different in the Magellanic Cloud clusters, where the available surveys are sensitive down to $M_{\rm bol} = -4.0$ and find many M stars but no S stars in the range -4.0 to -4.4. Does this mean that Tc-poor, extrinsic S stars are really absent from the Magellanic Cloud globular clusters? Possibly, although extrinsic S stars are mostly found at luminosities fainter than $M_{\rm bol} = -3.5$ (i.e. below the RGB-tip), and were thus not properly surveyed in the Magellanic Cloud clusters. The absence of extrinsic S stars in the Magellanic Cloud clusters would not be surprising, though, given the situation encountered in galactic globular clusters. Barium and (low-luminosity) S stars are rare in galactic globular clusters (Vanture et al. 1994, and references therein). They are only present in the massive, low-concentration cluster ω Cen (Lloyd Evans 1983b), and their origin in that cluster is still unclear. Côté et al. (1997) have argued that the binary evolution leading to the formation of extrinsic heavy-element-rich stars is only possible in low-concentration clusters like ω Cen. In more concentrated clusters, hard binaries rapidly shrink to orbital separations not large enough to accommodate an AGB star. It would be of interest to check whether Magellanic Cloud globular clusters are indeed too concentrated to allow the formation of extrinsic S stars. However, the recent result that the barium and the low-luminosity S stars in ω Cen appear to have constant radial velocities (Mayor et al. 1996) challenges the above picture. It may indicate that the barium and low-luminosity S

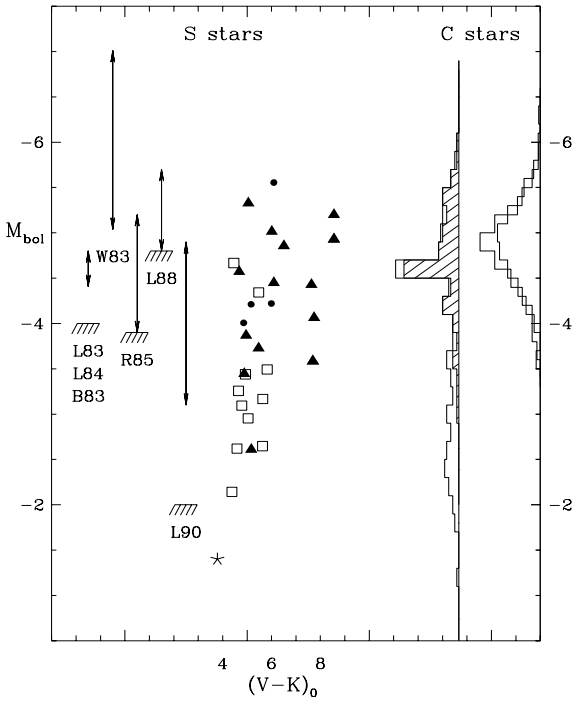

Fig. 7. Comparison of the $M_{\rm bol}$ range of S stars in the solar neighbourhood (this work, symbols are as in Fig. 2) and in external systems:
• **S stars**: LMC clusters: L83 (Lloyd Evans 1983a), L84 (Lloyd Evans 1984), B83 (Bessell et al. 1983); Magellanic Cloud fields: W83 (Wood et al. 1983), R85 (Reid & Mould 1985), L88 (Lundgren 1988); Fornax dwarf elliptical galaxy: L90 (Lundgren 1990). Detection thresholds are also indicated.
• **C stars**: the rightmost histogram gives the luminosity function of the 186 LMC (thick line) and 134 SMC (thin line) C stars identified by Blanco et al. (1980), adopting 18.6 for the LMC distance modulus and 0.5 mag as the difference in distance moduli between the Clouds. The leftmost histogram provides the luminosity functions of C stars from the Westerlund et al. (1991) SMC survey (hatched) as well as from the deeper Westerlund et al. (1995) SMC survey (open)

stars in ω Cen represent the extreme tail of the wide range in metal abundances observed in that particular globular cluster, as suggested by Lloyd Evans (1983b). Alternatively, these stars might have been enriched in the past by mass transfer in soft binary systems which were later dynamically disrupted.

The lack of low-luminosity S stars in the Fornax dwarf elliptical galaxy (L90 in Fig. 7) is probably related to the low-metallicity of that system ([Fe/H] ~ -1.5; Lundgren 1990). At such low metallicities, the red giant branch is shifted towards the blue, so that stars with luminosities typical of the galactic Tc-poor S stars are actually of spectral type G or K in Fornax (see Smith et al. 1996, 1997 for a discussion on a similar situation in the galactic halo). No specific effort to find heavy-element-rich stars among the warm ('continuum') giants was attempted by Lundgren (1990). Contrarily to the situation prevailing in the Magellanic Cloud clusters discussed above, an S star is found in Fornax at the luminosity threshold ($M_{\rm bol} = -3.2$) between 'continuum' (G or K) giants and M giants, suggesting that the lower luminosity cutoff observed for S stars in Fornax is just a spectral selection effect.

Deeper surveys are available for carbon stars, because of their more conspicuous spectral features. The luminosity distribution of the 134 SMC and 186 LMC carbon stars identified by the pioneering survey of Blanco et al. (1980) is shown in Fig. 7. It should be noted that the luminosity functions are almost identical for the LMC and SMC despite their different metallicities, so that the comparison with a more metal-rich galactic sample is not unreasonable. A GRISM survey of carbon stars in the SMC by Rebeirot et al. (1993; RAW) led to the discovery of 1707 such stars. For 100 of them, bolometric magnitudes were determined from JHK photometry (Westerlund et al. 1991), with a limiting magnitude of $M_{\rm bol} \sim -3$. Their distribution is represented by the hatched histogram on Fig. 7. A subsequent photometric and spectroscopic survey has been devoted to the $\sim 5\%$ among RAW objects having $M_{\rm bol} > -3$ (Westerlund et al. 1995; Fig. 7). *The range of absolute bolometric magnitudes for carbon stars from the deeper SMC survey now totally covers that of galactic S stars, including its low-luminosity tail.*

The nature of the SMC low-luminosity carbon stars is still debated. They might either be contaminating *dwarf* carbon (dC) stars from our own Galaxy, or low-luminosity carbon stars equivalent to the galactic R carbon stars, or may be extrinsic carbon stars formed by mass transfer across a binary system like galactic extrinsic S stars (as already suggested by Barnbaum & Morris 1993). Westerlund et al. (1995) reject the first hypothesis, mainly because none (except two) of their carbon stars have colours similar to the known galactic dC stars, and moreover, none exhibits a strong C_2 band head at 619.1 nm, a feature exhibited by galactic dC stars. The last two hypotheses offer interesting alternatives that remain to be investigated. It should also be noted that the possibility that some of the low-luminosity SMC carbon stars be extrinsic carbon stars makes it difficult to use the SMC carbon-star luminosity distribution to derive the luminosity threshold for the occurrence of the s-process and third dredge-up along the AGB (see the discussion in Sect. 4.2). Further observations are clearly required in order to distinguish intrinsic carbon stars from possible extrinsic carbon stars.

5. Infrared excess and position along the giant branches

Infrared excesses revealing the presence of cool circumstellar material are a common feature of late-type giants (e.g., van der Veen & Habing 1988; Habing 1996). These excesses are often associated with intrinsic stellar variability. Hacking et al. (1985) have shown that the brightest IRAS 12μm sources outside the galactic plane are long-period variables (LPV). Similarly, in globular clusters, all stars with a 10 μm excess are LPVs (Frogel & Elias 1988), and moreover, they are found only above the RGB tip. These IR excesses are associated with a strong mass loss, which thus appears to be the rule among LPVs. It is expected to be much smaller in non-pulsating AGB and RGB stars (e.g., Habing 1987). Consequently, S stars with large photometric variability and infrared excesses are expected to be found

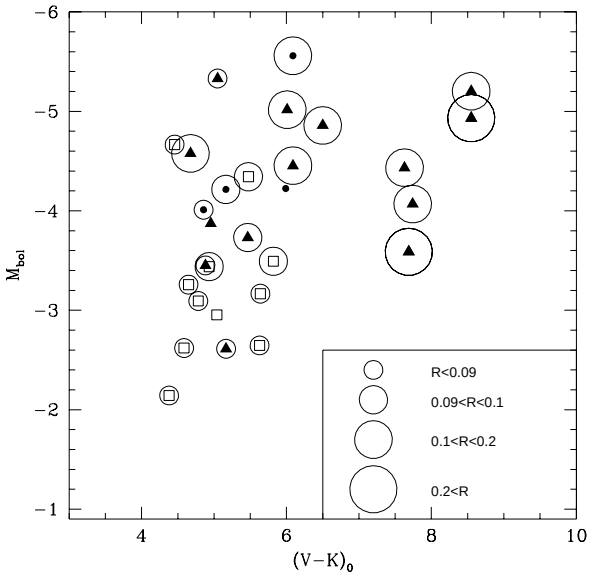

Fig. 8. Infrared excess along the giant branches, as measured by the ratio $R = F(12\mu\text{m})/F(2.2\mu\text{m})$. The dichotomy between extrinsic and intrinsic S stars is clearly apparent. Symbols are as in Fig. 2

among the most luminous stars. Indeed, it was already shown in Fig. 2 that variability in the HIPPARCOS Hp band tends to increase with luminosity. The present data offer the possibility to investigate as well the evolution of the IR excesses probing mass loss along the giant branches in the HR diagram.

The ratio $R = F(12\mu\text{m})/F(2.2\mu\text{m})$, probing the presence of cool circumstellar material emitting at 12 μm, has been derived from the IRAS PSC and from the K magnitude, whenever available (using the calibration of Beckwith et al. 1976 to convert K magnitudes into fluxes at 2.2 μm). As already shown by Jorissen et al. (1993), there is a clear segregation of S stars according to their value of R. All Tc-deficient S stars have $0.075 \lesssim R \lesssim 0.093$, consistent with photospheric blackbody colours (R = 0.073 for $T_{\rm eff}$= 4000 K and R = 0.093 for $T_{\rm eff}$= 3150 K, which corresponds to the $T_{\rm eff}$ range spanned by extrinsic S stars). On the contrary, intrinsic S stars generally have $R > 0.1$, indicative of circumstellar dust. This segregation is a further indication of the inhomogeneous nature of the family of S stars.

As expected, Fig. 8 clearly shows that $R < 0.1$ indices are restricted to the RGB (or E-AGB), whereas S stars on the AGB have larger and larger R indices as they evolve towards cooler $T_{\rm eff}$.

6. Conclusions

All stars with ZrO bands were historically assigned to a unique spectral class (S). However, an increasing number of arguments recently suggested that the S family comprises stars of two different kinds: Tc-poor binary (extrinsic) S stars and Tc-rich (intrinsic) S stars. The HR diagram of S stars constructed from HIPPARCOS parallaxes presented in this study fully confirms that dichotomy, by showing that:

- extrinsic S stars are hotter and intrinsically fainter than intrinsic S stars;
- extrinsic S stars are low-mass stars populating either the RGB or the E-AGB, and in any case are found *below* the luminosity threshold marking the onset of thermal pulses on the AGB. Therefore, their chemical peculiarities cannot originate from internal nucleosynthesis and dredge-up processes occurring along the TP-AGB. Their binary nature suggests instead that their chemical peculiarities originate from mass transfer;
- on the contrary, Tc-rich S stars are found just above the TP-AGB luminosity threshold. Their location in the HR diagram indicates that s-process nucleosynthesis and third dredge-up must be operative quite early on the TP-AGB.

The galactic latitude distributions of extrinsic and intrinsic S stars are also clearly different (Jorissen et al. 1993; Jorissen & Van Eck 1997), indicating that they are not simply successive stages along the evolution of stars in the same mass range.

Acknowledgements. We would like to thank F. Pont for useful discussions. S.V.E. is supported by a F.R.I.A. (Belgium) doctoral fellowship, and A.J. is Research Associate (F.N.R.S., Belgium). Financial support from the *Fonds National de la Recherche Scientifique* (Belgium, Switzerland) is gratefully acknowledged. This research has made use of the *General Catalogue of Photometric Data*, operated at the Institute of Astronomy, University of Lausanne (Switzerland) and of the SIMBAD database, operated at CDS, Strasbourg (France).

Appendix A: 57 Peg: a very luminous extrinsic S star

The star 57 Peg is peculiar in being a high-luminosity extrinsic S star ($M_{\rm bol}$= −4.3; Table 2). Its outlying position cannot be attributed to the uncertainty on its parallax, which is small (σ_π/π = 0.21; Fig. 4). It is a long-period binary system ($P > 3700$ d; Jorissen et al. 1997a) with a composite spectrum caused by a companion of spectral type approximately A3V, as derived by Hackos & Peery (1968) from the analysis of a violet optical spectrum. The A-type main sequence companion is much better visible on the IUE spectra available in the archive (Peery 1986). In order to derive its exact spectral class, and thus its mass, its UV colours were compared to standard stars from the atlas of Wu et al. (1983). Fig. A1 presents the location of 57 Peg in the $([17]-[18],[17]-[19])$ colour-colour diagram, where $[i]-[j] = -2.5\log(F_i/F_j)$ and F_i is the average flux in the spectral ranges 165.5 – 175.5 nm (for i = 17), 175.5 – 185.5 nm (i = 18) or 185.5 – 195.5 nm (i = 19). All the stars from the atlas of Wu et al. (1983) plotted on Fig. A1 have a flux well above the noise level in all three bands. For 57 Peg, the two spectra used (SWP05384, recorded on May 28, 1979 and SWP32554, obtained on December 18, 1987) yield identical colours, despite the fact that they were obtained about 8 years apart. All spectra were retrieved from the final IUE archive processed with the NEWSIPS software. No reddening correction has been applied, since it is assumed to be negligible given the small colour excesses listed by Wu et al. (1983) and by Hackos & Peery (1968).

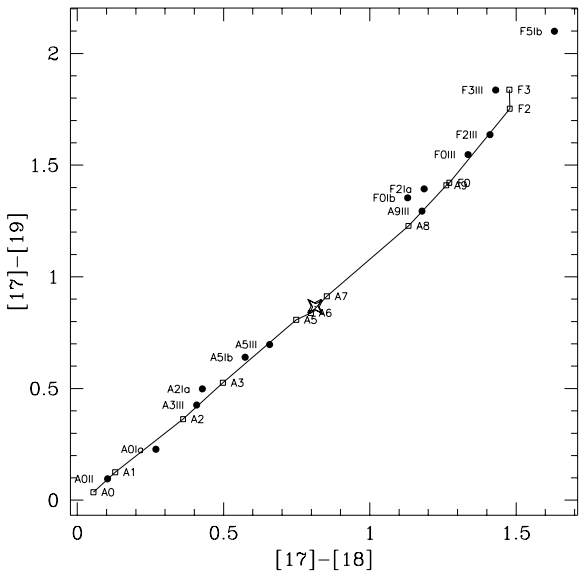

Fig. A1. The ([17]−[18], [17]−[19]) colour-colour diagram for 57 Peg (cross) and standard stars from the spectral atlas of Wu et al. (1983). Main sequence stars are represented by open squares with labels on the right giving the corresponding *optical* spectral type. Giants and supergiants are represented by filled circles, with labels on the left of the corresponding point

Main sequence stars fall along a straight line in Fig. A1, with 57 Peg falling around spectral type A6. Although the colour-colour diagram does not probe efficiently the luminosity class, the individual fluxes of 57 Peg are compatible with the companion being an A6 star on the main sequence, since its fluxes match those of the A6V standard HD 28527 (SWP19459), assuming $M_{\rm v}$ = +2.05 for A6V stars, and given the distance derived for the 57 Peg system from the HIPPARCOS parallax. The corresponding mass for the companion is then 1.9 $M_\odot$. The S star primary must have evolved faster and should thus be more massive than 1.9 $M_\odot$, which is consistent with its position in the HR diagram along the 3 $M_\odot$ E-AGB (Fig. 6). That S star is thus likely to be more massive than the average extrinsic S star (for which $\langle M \rangle$ = 1.6±0.2 $M_\odot$; Sect. 4.2 and Jorissen et al. 1997a).

The Tc-poor nature of 57 Peg is quite puzzling, though, since the binary paradigm (Sect. 1) requires the companion of a Tc-poor S star to be a WD rather than a main sequence star. Possibilities to resolve this puzzle within the framework of the binary paradigm for extrinsic S stars include (i) 57 Peg is a triple system (S+A6V+WD), or (ii) the companion is an accreting WD mimicking a main sequence spectrum, or (iii) 57 Peg is not an S star at all. The radial-velocity data accumulated so far does not allow us to test possibility (i) yet. Possibility (ii) is unlikely, since the SWP spectrum carries no sign of binary interaction (like the CIV λ155.0 doublet), the two spectra taken 8 years apart yield identical fluxes (whereas some variability is expected in the case that the observed continuum be due to accretion on a WD), and finally, in the regime of rapid mass accretion by a WD, where a stable H-burning shell forms, the accreting WD mimics a supergiant rather than a main sequence star (e.g., Paczyński & Rudak 1980). Possibility (iii) - 57 Peg is not an S star - has already been mentioned explicitly by Smith & Lambert (1988) with reference to an earlier paper (Smith & Lambert 1986), although 57 Peg is not to be found in that other paper. This last possibility clearly deserves a closer study. Otherwise, 57 Peg would add to the small set of Tc-poor S stars (HD 191589, HDE 332077) with a main sequence companion (Jorissen & Mayor 1992; Ake & Johnson 1992; Ake et al. 1994; Jorissen et al. 1997a).

Appendix B: an evaluation of the impact of statistical biases

The evaluation of the statistical biases altering the true absolute magnitude distribution of any given observed sample of stars requires the knowledge of the selection criteria defining that sample. Indeed, magnitude-limited samples are mostly affected by the Malmquist bias (Malmquist 1936), whereas the Lutz-Kelker bias plays an important role for parallax-limited samples (e.g. Lutz & Kelker 1973; Lutz 1979; Hanson 1979; Smith 1988). For the HIPPARCOS sample of S stars considered here, the selection criteria combine limits on the parallax with limits on the magnitude. Monte-Carlo simulations (see e.g. Pont et al. 1997) appear therefore more appropriate than an analytical approach to explore the biases resulting from the selection criteria and the observation errors when applied to a reasonable model of the parent population.

The main aim of the simulations presented in this Appendix is to demonstrate that the segregation observed in the HR diagram between Tc-rich and Tc-poor S stars is not an artefact caused by statistical biases which might in principle operate differentially on the two families (because e.g. of different galactic distributions), but that it must result instead from truly different luminosity distributions.

To this aim, a parent population of *Tc-rich* S stars is generated with the following properties:

- a large number ($>$ 300 000) of Tc-rich S stars are created, with a spatial distribution characterized by an exponential scale height of 180 pc (as derived for the Tc-rich stars of the Henize sample comprising 205 S stars; Van Eck & Jorissen, in preparation), and a uniform projected distribution on the galactic plane around the Sun;
- various bolometric-magnitude distributions are adopted (see below);
- the $(V-I)_{\rm J}$ colour index is derived from the bolometric magnitude using a fiducial AGB fitted to our sample:

$$(V-I)_{\rm J} = (0.5 - M_{\rm bol})/1.5 + \sigma_{\rm V-I}\ {\rm gauss}(0,1) \qquad \text{(B1)}$$

  where $\sigma_{\rm V-I}$ = 0.6 and gauss(0,1) is a random variable with a reduced normal distribution;
- the bolometric correction is computed from the $(BC_{\rm I}, (V-I)_{\rm J})$ relation of Bessell & Wood (1984);
- the (unreddened) $V_{\rm J,0}$ magnitude is deduced from the distance d, $M_{\rm bol}$, $BC_{\rm I}$ and $(V-I)_{\rm J}$;
- the $V_{\rm J,0}$ magnitude is reddened according to the cosecant formula (Feast et al. 1990).

Stars are extracted from this parent population so as to reproduce the *observed* distribution of V_J magnitudes in the entire[2] HIPPARCOS sample of S stars. The "measured" parallax of each extracted star is then computed from its distance d by

$$\pi_{\rm measured} = 1/d + \sigma_\pi(V_J)\ {\rm gauss}(0,1) \qquad \text{(B2)}$$

where the (σ_π, V_J) relationship is derived from a least square fit to the HIPPARCOS data for S stars. The simulated star is then retained if it satisfies the condition $0 < \sigma_\pi/\pi < 0.85$ imposed on the star in order to be included in the HR diagram of Fig. 2.

In summary, the two selection criteria are:

- Condition I: the V_J distribution of the extracted sample of simulated stars has to reproduce the V_J distribution of the HIPPARCOS sample of S stars;
- Condition II: $0 < \sigma_\pi/\pi < 0.85$.

The stars extracted from the parent population and satisfying condition I (resp. I+II) define what will be called in the following the sample $\Sigma_{\rm I}$ (resp. $\Sigma_{\rm I+II}$). The sample $\Sigma_{\rm I}$ is supposed to represent the real HIPPARCOS sample.

Although the selection criteria that were used to include a given S star in the HIPPARCOS Input Catalogue are unknown to us, condition I ensures that they are implicitly met in our simulation. Besides, condition II is satisfied by 61% of the stars in $\Sigma_{\rm I}$ to be compared with 63% in the real HIPPARCOS sample of S stars. This good agreement constitutes a check of the internal consistency of our model as a whole.

The comparison between the $M_{\rm bol}$ distributions of the sample $\Sigma_{\rm I+II}$ and of the parent sample then illustrates the impact of the statistical biases. This is shown in Fig. B1 for rectangular parent distributions in the range $-4 \geq M_{\rm bol} \geq -6$ (Fig. B1a) and in the range $-2 \geq M_{\rm bol} \geq -6$ (Fig. B1b). The net effect of these biases is to transform the original rectangular distribution into a bell-shaped distribution, with a median shifted by 0.4 magnitude towards fainter objets, and with asymmetrical tails extending beyond the original limits. This spread is most pronounced on the fainter side of the distribution. The faintest *observed* S star in a sample of N objects must therefore be expected beyond the lower boundary of the *parent* distribution (at a bolometric magnitude corresponding to the cumulative frequency $1/N$). The amplitude of this offset does not depend on the median value of the parent distribution, but depends rather sensitively upon its width (compare Fig. B1a and Fig. B1b). For reasonable values of the width of this parent $M_{\rm bol}$ distribution, and adopting $N = 14$ as for the sample of Tc-rich S stars plotted in the HR diagram of Fig. 4, the offset value is found to lie between 0.7 and 1.5 mag. According to this statistics, the presence of the Tc-rich S star NQ Pup at $M_{\rm bol} = -2.6$ (i.e. about 1 mag below the onset of the TP-AGB) is nevertheless fully compatible with its location on the TP-AGB (see Fig. 6). Furthermore,

[2] The V_J distribution of the entire HIPPARCOS sample of S stars (60 stars when excluding the two close visual binaries and the misclassified S star; see Table 1) has been preferred over the V_J distribution of the 21 S stars known to be Tc-rich, because of its larger statistical significance and because the observed V_J distributions of Tc-rich and Tc-poor S stars are not significantly different.

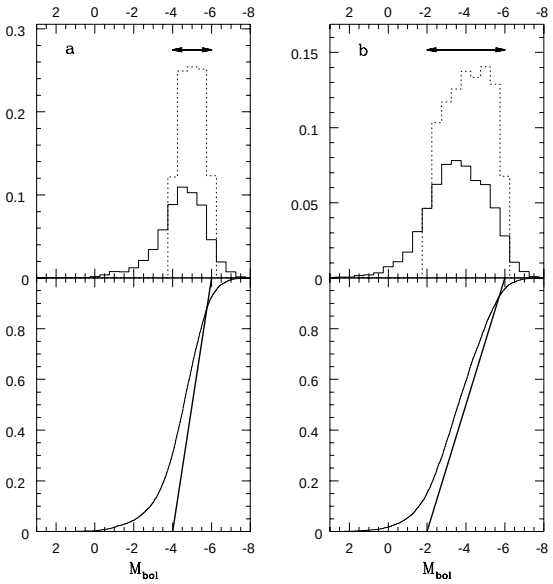

Fig. B1. Bolometric magnitude distributions (upper panels) and their cumulative frequencies (lower panels) resulting from the Monte-Carlo simulations described in the text. The *parent* $M_{\rm bol}$ distributions are rectangular and span the range indicated by the arrows in the upper panels. In the lower panel, their cumulative frequency is represented by the thick solid line. The dotted line (resp. thin solid line) refers to the distribution of the $\Sigma_{\rm I}$ (resp. $\Sigma_{\rm I+II}$) sample. Both histograms are drawn at the same scale, the dotted histogram being normalized to unity. Note that a Malmquist-type bias is responsible for the deviation of the dotted histogram from the original rectangular distribution, whereas a Lutz-Kelker-type bias causes the difference between the dotted- and the thin-solid histograms

Fig. B1b demonstrates *ad absurdum* that the luminosity segregation between Tc-rich and Tc-poor S stars is not an artefact: if Tc-rich S stars with $-2 \geq M_{\rm bol} \geq -4$ typical of Tc-poor S stars were to exist, they should have been detected indeed.

Two conclusions may thus be drawn from the above simulations:

- they demonstrate that the lack of low-luminosity Tc-rich S stars does not result from statistical biases, since these biases tend to *increase* the number of low-luminosity stars;
- when inferring the luminosity threshold for the appearance of Tc-rich S stars, it must be reminded that statistical biases tend to make the faintest Tc-rich S stars observed by HIPPARCOS appear *below* (between 0.7 and 1.5 mag) the true lower-luminosity boundary of the parent population.

References

Aaronson M., Mould J., Cook K.H., 1985, ApJ 291, L41

Ake T.B., Johnson H.R., 1992. In: Giampapa M.S., Bookbinder J.A. (eds.) Seventh Cambridge Workshop on Cool Stars, Stellar Systems and the Sun. Astron. Soc. Pacific Conf. Series 26, p. 579

Ake T., Jorissen A., Johnson H.R., Mayor M., Bopp B., 1994, Bull. Am. Astron. Soc. 24, 1280

Arenou F., Lindegren L., Froeschle M., Gomez A.E., Turon C., Perryman M.A.C., Wielen R., 1995, A&A 304, 52

Barnbaum C., Morris M., 1993, Bull. American Astron. Soc., 182, #46.17
Beckwith S., Evans N.J., Becklin E.E., Neugebauer G., 1976, ApJ 208, 390
Bessell M.S., Wood P.R., Lloyd Evans T., 1983, MNRAS 202, 59
Bessell M.S., Wood P.R., 1984, PASP 96, 247
Bidelman W.P., Keenan P.C., 1951, ApJ 114, 473
Blanco V.M., McCarthy M.F., Blanco B.M., 1980, ApJ 242, 938
Boesgaard A.M., 1969, PASP 81, 283
Böhm-Vitense E., Nemec J., Proffitt C., 1984, ApJ 278, 726
Brewer J.P., Richer H.B., Crabtree D.R., 1996, AJ 112, 491
Brown J.A., Smith V.V., Lambert D.L., Dutchover E.Jr., Hinkle K.H., Johnson H.R., 1990, AJ 99, 1930
Brown A.G.A., Arenou F., van Leeuwen F., Lindegren L., Luri X., 1997. In: Perryman M.A.C. (ed.) The Hipparcos and Tycho Catalogues, ESA-SP 402, in press
Burstein D., Heiles C., 1982, AJ87, 1165
Catchpole R.M., Feast M.W., 1976, MNRAS 175, 501
Catchpole R.M., Robertson B.S.C., Lloyd Evans T.H.H., Feast M.W., Glass I.S., Carter B.S., 1979, SAAO Circ. 1, 61
Charbonnel C., Meynet G., Maeder A., Schaerer D., 1996, A&AS 115, 339
Chen P. S., Gao H., Chen Y. K., Dong H. W., 1988, A&AS 72, 239
Cohen J.G., Frogel J.A., Persson S.E., Elias J.H., 1981, ApJ 249, 481,
Côté P., Hanes D.A., McLaughlin D.E., Bridges T.J., Hesser J.E., Harris G.L.H., 1997, ApJ 476, L15
Culver R.B., Ianna P.A., 1975, ApJ 195, L37
Eggen O.J., 1972a, PASP 84, 406
Eggen O.J., 1972b, ApJ 177, 489
ESA, 1997. The HIPPARCOS Catalogue, ESA SP-1200
Eyer L., Grenon M., 1997. In: Perryman M.A.C. (ed.) The Hipparcos and Tycho Catalogues, ESA-SP 402, in press
Feast M.W., 1953, MNRAS 113, 510
Feast M.W., Catchpole R.M., Glass I.S., 1976, MNRAS 174, 81P
Feast M.W., Robertson B.S.C., Catchpole R.M., Lloyd Evans T., Glass I.S., Carter B.S., 1982, MNRAS 201, 439
Feast M.W., Whitelock P.A., Carter B.S., 1990, MNRAS 247, 227
Fouqué P., Le Bertre T., Epchtein N., Guglielmo F., Kerschbaum F., 1992, A&AS 93, 151
Frogel J.A., Elias J.H., 1988, ApJ 324, 823
Gillett F.C., Merrill K.M., 1971, ApJ 164, 83
Habing H.J., 1987. In: Appenzeller I., Jordan C. (eds.) Circumstellar Matter (IAU Symp. 122). Reidel, Dordrecht, p.197
Habing H.J., 1996, ARA&A 7, 97
Hacking P., Neugebauer G., Emerson J., et al., 1985, PASP 97, 616
Hackos W.Jr., Peery B.F.Jr., 1968, AJ 73, 504
Hakkila J., McNamara B.J., 1987, A&A 186, 255
Hanson R.B., 1979, MNRAS 186, 875
Henize K.G., 1960, AJ 65, 491
Houk N., Cowley A.P., 1975. The Michigan Catalogue of Two-Dimensional Spectral Types for the HD Stars. Univ. Michigan, Ann Arbor, Vol. 1
Iben I.Jr., Renzini A., 1983, ARA&A 21, 271
IRAS Science Team, 1988. IRAS Point Source Catalogue, prepared by Beichman C.A., Neugebauer G., Habing H.J., Clegg P.E., Chester T.J., NASA-RP 1190
Jaschek C., 1978, Bull. Inf. CDS 15
Jaschek C., Jaschek M., 1987. The Classification of Stars, Cambridge Univ. Press
Johnson H.L., 1966, ARA&A 4, 193
Johnson H.R., Ake T.B., Ameen M.M., 1993, ApJ 402, 667
Jorissen A., Mayor M., 1992, A&A 260, 115
Jorissen A., Frayer D.T., Johnson H.R., Mayor M., Smith V.V., 1993, A&A 271, 463
Jorissen A., Knapp G.R., 1997, A&A, in press
Jorissen A., Van Eck S., 1997. In: Wing R. (ed.) The Carbon Star Phenomenon (IAU Symp. 177). Kluwer, Dordrecht, in press
Jorissen A., Van Eck S., Mayor M., Udry S., 1997a, A&A, submitted
Jorissen A., Mowlavi N., Sterken C., Manfroid J., 1997b, A&A 324, 578
Käppeler F., Beer H., Wisshak K., 1989, Rep. Prog. Phys. 52, 945
Keenan P.C., 1950, AJ 55, 172
Keenan P.C., 1954, ApJ 120, 484
Kholopov P.N., Samus' N.N., Frolov M.S., et al., 1985, General Catalogue of Variable Stars (4th edition), Moscow, Nauka
Koornneef J., 1983, A&A 128, 84
Lindegren L., 1995, A&A 304, 61
Little S.J., Little-Marenin I.R., Hagen-Bauer W., 1987, AJ 94, 981
Lloyd Evans T., 1983a, MNRAS 204, 985
Lloyd Evans T., 1983b, MNRAS 204, 975
Lloyd Evans T., 1984, MNRAS 208, 447
Lloyd Evans T., Catchpole R.M., 1989, MNRAS 237, 219
Lü P.K., 1991, AJ 101, 2229
Lundgren K., 1988, A&A 200, 85
Lundgren K., 1990, A&A 233, 21
Luri X., Arenou F., 1997. In: Perryman M.A.C. (ed.) The Hipparcos and Tycho Catalogues, ESA-SP 402, in press
Lutz T.E., 1979, MNRAS 189, 273
Lutz T.E., Kelker D.H., 1973, PASP 85, 573
Malmquist K.G., 1936, Stockolms Obs. Medd. No. 26
Mathews G.J., Takahashi K., Ward R.A., Howard W.M., 1986, ApJ 302, 410
Mavridis L.N., 1960, PASP 72, 48
Mayor M., Duquennoy A., Udry S., Andersen J., Nordström B., 1996. In: Milone E.F., Mermilliod J.Cl. (eds.) The Origins, Evolution, and Destinies of Binary Stars in Clusters. ASP Conf. Ser., San Francisco, p. 190
McClure R.D., 1984, PASP 96, 117
McClure R.D., Woodsworth A.W., 1990, ApJ 352, 709
Mennessier M.-O., Luri X., Figueras F., Gómez, A.E., Grenier S., Torra J., 1997, A&A, in press
Merrill P.W., 1922, ApJ 56, 457
Merrill P.W., 1952, ApJ 116, 21
Miller G.E., Scalo J., 1982, ApJ 263, 259
Mould J., Aaronson M., 1986, ApJ 303, 10
Neckel Th., Klare G., 1980, A&AS 42, 251
Neugebauer G., Leighton R.B., 1969. Two-Micron Sky Survey, NASA SP-3047 (TMSS)
Noguchi K., Sun J., Wang G., 1991, PASJ 43, 275
Pont F., Mayor M., Turon C., VandenBerg D.A., 1997, A&A, submitted
Paczyński B., Rudak B., 1980, A&A 82, 349
Peery B.F.Jr., 1986. In: New Insights in Astrophysics. ESA-SP 263, p.117
Price S.D., Murdock T.L., 1983. The Revised AFGL Infrared Sky Survey Catalog (AFGL-TR-83-0161)
Rebeirot E., Azzopardi M., Westerlund B.E., 1993, A&AS 97, 603
Reid N., Mould J., 1985, ApJ 299, 236
Richer H.B., 1981, ApJ 243, 744
Ridgway S.T., Joyce R.R., White N.M., Wing R.F., 1980, ApJ 235, 126
Sackmann I.-J., Boothroyd A.I., 1991. In: Michaud G., Tutukov A. (eds.) Evolution of Stars: The Photospheric Abundance Connection (IAU Symp. 145). Kluwer, Dordrecht, p. 275

Scalo J.M., 1976, ApJ 206, 474
Scalo J.M., Miller G.E., 1981, ApJ 246, 251
Schaller G., Schaerer G., Meynet G., Maeder A., 1992, A&AS 96, 269
Smith H.Jr., 1988, A&A 198, 365
Smith V.V., Lambert D.L., 1986, ApJ 311, 843
Smith V.V., Lambert D.L., 1988, ApJ 333, 219
Smith V.V., Lambert D.L., 1990, ApJS 72, 387
Smith V.V., Plez B., Lambert D.L., Lubowich D.A., 1995, ApJ 441, 735
Smith V.V., Cunha K., Jorissen A., Boffin H.M.J., 1996, A&A 315, 179
Smith V.V., Cunha K., Jorissen A., Boffin H.M.J., 1997, A&A 324, 97
Stein R.W., 1991, ApJ 377, 669
Stephenson C.B., 1984. The General Catalogue of Galactic S Stars, Publ. Warner & Swasey Observ. 3, 1
Takayanagi W., 1960, PASJ 12, 314
Turon C. et al., 1992a. The HIPPARCOS Input Catalogue, ESA SP-1136
Turon C. et al., 1992b, Bull. Inform. CDS 41, 9
Turon C. et al., 1992c, Bull. Inform. CDS 43, 5
van der Veen W.E.C.J., Habing H.J., 1988, A&A 194, 125
van Leeuwen F., Feast M.W., Whitelock P.A., Yudin B., 1997, MNRAS 287, 955
Vanture A.D., Wallerstein G., Brown J.A., 1994, PASP 106, 835
Warner B., 1965, MNRAS 129, 263
Wagenhuber J., Tuchman Y., 1996, A&A 311, 509
Westerlund B.E., Olander N., Hedin B., 1981, A&AS 43, 267
Westerlund B.E., Azzopardi M., Breysacher J., Rebeirot E., 1991, A&AS 91, 425 (with erratum in A&AS 92, 683)
Westerlund B.E., Azzopardi M., Breysacher J., Rebeirot E., 1995, A&A 303, 107
Willems F.S., de Jong T., 1986, ApJ 309, L39
Wing R. F., Yorka, S. B., 1977, MNRAS 178, 383
Wood P.R., Bessell M.S., Fox M.W., 1983, ApJ 272, 99
Wu C.-C., Ake T.B., Boggess A., Bohlin R.C., Imhoff C.L., Holm A.V., Levay Z.G., Panek R.J., Chiffer F.H.III, Turnrose B.E., 1983. The Ultraviolet Spectral Atlas, NASA IUE Newsletter 22
Yorka S.B., Wing R.F., 1979, AJ 84, 1010

This article was processed by the author using Springer-Verlag LaTeX A&A style file *L-AA* version 3.